ACTA STEREOL 1999; 18/2: 227-237
ORIGINAL SCIENTIFIC PAPER

CHARACTERISATION OF DIFFUSION PATHS OF WATER IN CONCRETE BY COLOR IMAGE ANALYSIS

Anne-Sophie Dequiedt, Carl Redon, Jean-Louis Chermant, Liliane Chermant, Michel Coster

LERMAT, UPRESA CNRS 6004, ISMRA, 6 Bd Maréchal Juin, 14050 Caen Cedex, France

ABSTRACT

The scope of this paper is to investigate the dispersion of air-voids in concrete. Different automatic methods of image analysis are proposed to characterise this dispersion and the distribution of path lengths from given points of the cement paste to the air-voids, using euclidean or geodesic processes. It is shown that the distances between air-voids increase with gravel content and that geodesic distances are higher than the euclidean ones.

Key words: concrete, air-voids, path length, mathematical morphology, euclidean distance, geodesic distance.

INTRODUCTION

A concrete is composed of several phases: the gravel, the cement and pores. Moreover the cement paste is, itself, constituted of several crystalline phases. For civil engineering materials, the notion of pores is complex: it can include i) a large number of air-voids whose size varies from some micrometers to several millimeters, and ii) pores and capillarities corresponding to a very small scale (some nanometers). The air-voids correspond to entrapped air during the mixing and process route (Whiting and Stark, 1983; Mielenz *et al.*, 1958). They are connected with the network of capillary pores in the hardened cement paste. The presence of this connected network (capillary pores and air-voids) in concrete has a great influence on the frost resistance of these materials (ATHIL, 1989). This one depends on the volume fraction of air-voids, their size distribution and their dispersion in the concrete. Indeed, upon freezing, the free water present in the porous system moves inside this porous set to air-voids where there is formation of ice (Powers, 1949; Powers and Helmuth, 1953; Powers, 1954). The distance for the water to reach a void is therefore an important parameter to study the frost resistance of concrete.

Due to the large size distribution of voids, the best parameter to investigate is generally the half-distance between voids (Mielenz *et al.*, 1958; Powers, 1954; Pigeon and

Lachance, 1981). We can note that this parameter differs from the one chosen by the AFNOR norm NF 480-11, which estimates the dispersion by the mean free path in one direction of analysis.

Before studying the water path in concrete, the different phases must be defined by some stereological parameters. Then, for the present study, we can consider that water cannot move through the gravel. So, the distance between air-voids can be studied by two ways : euclidean or geodesic distances. Moreover if a finer analysis of the voids dispersion is weshed, the distribution of these distances is important to know. The goal of this paper is to propose automatic methods to analyse these distances between voids, to compare these different methods and to get some results as a function of gravel content.

TESTED MATERIALS AND SAMPLE PREPARATION

For this study, three different concrete have been fabricated, (Table I). On the video screen, the gravel used appears in "red", with a granulometry between 3.5 and 6.3 mm, while that of the sand is limited to 4 mm.

Table I: Composition of the different studied concrete.

batch	Cement [g/l]	gravel + sand			water/cement (by weight)
		total g/l	gravel [%]	sand [%]	
A	450	2000	60	40	0.5
B	450	2000	40	60	0.5
C	450	2000	20	80	0.5

Parallelepipedic specimens, 4 x 4 x16 cm^3 in size, were fabricated. After one month of drying, each specimen was cut in about twenty thick slices. These slices were embedded in a green fluorescence epoxy resin and then ground.

IMAGE PROCESSING

Acquisition of images

Images are obtained by putting sections of concrete on a scanner (Hewlett Packard ScanJet 4C). The coloured images are coded in 651 x 651 pixels in the Red-Green-Blue space with 256 levels by channel. The resolution was 31 pixels/mm. So, the gravel appear in "red" (R on figure 1), the cement in white (W on figure 1), the sand in brown (B on figure 1) and the air-voids (resin) in light green (G on figure 1).

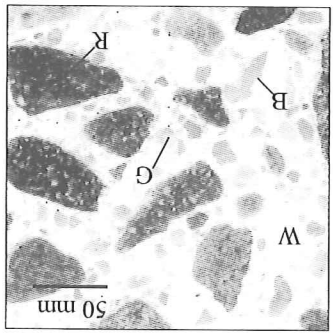

Figure 1 : RGB metallographic image of a slice of concrete : W : cement; R : gravel; G : air-voids; B : sand.

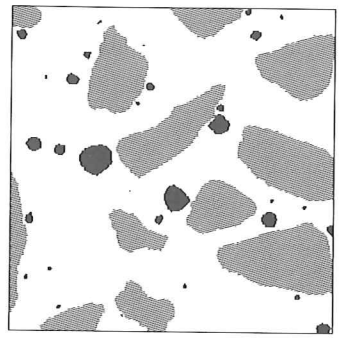

Figure 2 : Digitised image of the three regions.

Segmentation of the different regions of the concrete

Three regions (gravel, voids and the matrix (cement + sand)) are concerned for the segmentation.

The image of gravel is obtained from its complementary colour, i.e. the green component of the coloured image. This green image is filtered by a numerical closing of size 1. The binary image is then obtained by an automatic maximum contrast threshold (Kohler, 1981). The filtering process of this image is the following : i) an open-reconstruction to eliminate fine particles (sand) and ii) a hole filling (Figure 2 : grey zones).

To segment the air-voids is more difficult because, although they are full of resin, their colour depends on their depth. Their colour varies from yellow to green. So, it cannot be detected in the RGB space, because there is a recovery of the air-voids grey levels and this one of another phase. It is more practice to detect it on the component Q of the YIQ coloured space. The YIQ space is used by the National Television Standard Committee (NTSC) : it is obtained with a 3 x 3 revertible transformation matrix from RGB to YIQ (Kunt, 1991). With an automatic maximum contrast threshold on the component Q, the binary image of the air-voids is obtained. An open-reconstruction of size 1 and a hole filling are used to filter the binary image (Figure 2 : black zones).

Then the matrix image is the complement of the two previous images (Figure 2 : white zones).

PHASE CHARACTERISTIC

To characterise quantitatively these different phases, it necessitates to develop an automatic processing as there is a great number of images to analyse. The characterisation of each batch was performed from 40 images. Some stereological parameters (De Hoff and Rhines, 1972, Hadwiger, 1957) are presented in Table II.

Table II : Characterisation of gravel (Gr) and air-voids (AV) phases. V_V : volume fraction; N_A : connectivity number in R^2; $\bar{A}$: mean surface area.

Batch	gravel (Gr)			air-void (AV)		
	$V_V(Gr)$	$N_A(Gr)$	$A(Gr)_{mm^2}$	$V_V(AV)$	$N_A(AV)$	$A(AV)_{mm^2}$
A	0.4605	17	11.859	0.0078	17	0.209
B	0.3293	13	10.848	0.0205	20	0.448
C	0.145	6	10.380	0.0329	26	0.559

The mean surface area, $\bar{A}(Gr)$, of gravel is similar for the three types of samples : the gravel used for the three concrete specimens is the same. Their volume fraction, $V_V(Gr)$, and the connectivity number, N_A, vary with the proportion of gravel content in concrete (Table I).

The content and number of air-voids are inversely proportional to the gravel content. So in batch C, more voids are present than in batch A. The same variation is observed for the mean surface area, $\bar{A}(AV)$, of voids.

ANALYSIS OF THE VOIDS DISPERSION

To study the dispersion of air-voids, two approaches are possible. For the first one, the analysis is performed by an euclidean manner on all the image. For the second one, we consider that the water cannot move into gravel : so the analysis will be performed by a geodesic way in the complementary set of gravel (Lantuejoul and Beucher, 1981). In addition, the dispersion analysis can be made by several ways. In this study, the distribution of distances between neighbours was first used, and then the distance function (chess distance) (Rosenfeld and Pfaltz, 1968).

Methods 1 and 2: Distribution of distances between the nearest neighbours

Two approaches are proposed to investigate the distribution of distances between the nearest neighbours : i) the first one is realised from an individual analysis of voids; ii) the second one is performed from a global image analysis.

Method 1 : By *individual analysis*, the binary image of voids is labelled. Each void is independently dilated until to meet a void of the complete image. For the geodesic study, the studied void is dilated by a geodesic way in the complementary set of gravel. To take into account the local knowledge, the analysis is performed in a mask eroded by the maximum void size included in the image. Only voids whose centre is inside the mask are labelled. Several parameters for the distance distribution between the first neighbour are computed.

Method 2 : For the *global analysis*, a method derived from the Shehata's method (1989) was chosen. Its principle consists to calculate the number of particles that stay isolated after a certain number of dilations. The size of dilation corresponds to the half-distance that separates two voids. According to a topological point of view, the difference between dilated void and void itself gives an object of connectivity 0. This property and the property of homotopy of the complete thinning by the element D (Serra, 1982; Coster and Chermant, 1985; 1989) are used to isolate voids which are not connected by the dilation.

Indeed, only voids connected by dilation give thinned images with multiple points (Figure 3). These multiple points will be used to serve as markers to reconstruct connected voids, and by difference isolated voids. Thus, to each dilation the number of un-connected particles is recorded. Its variation allows to obtain the distribution of individual particles which disappear as a function of the dilation size. From this distribution, the same parameters as before are extracted. A geodesic version of this algorithm has been developed: the euclidean dilation is then replaced by a geodesic dilation of voids in the matrix. We call this method "count-dilation".

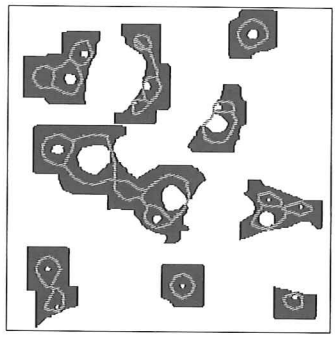

Figure 3 : Geodesic dilation of voids and their D skeleton.

Method 3 : Distribution of distances between all neighbours (SKIZ method)

The half-distance between voids can also be analysed by the distribution of distances from all neighbour voids to one given void. That corresponds to study the skeleton by influence zone (SKIZ) of voids. Thus, a reconstruction of segments of this SKIZ by successive dilations of air-voids is considered. After elimination of the SKIZ multiple points, the voids are dilated step by step by an euclidean or geodesic way. For the geodesic version, the geodesic SKIZ of voids in the complementary set of gravel is used. When a segment is reached, it is reconstructed and subtracted to the binary segments image. By iteration, all isolated segments are eliminated.

To each iteration, the number of reconstructed segments is recorded. The disappearance frequency of segments according to the dilation size is thus obtained. From its distribution, the same parameters as previously can be extracted.

Method 4 : Study of the dispersion from the distance function

The last utilised method is the distance function in the complementary set of the air-voids. It allows to characterise their dispersion. As explained in the introduction, distances in the complementary set of gravel is interesting regarding a physical point of view.

Therefore a geodesic version of this function with successive geodesic erosions has been used. However, the geodesic transformations can lead to a problem regarding the edge of the frame of measurements. To solve this problem we have used an adaptative mask in which measurements of geodesic distances are not biased. So the next steps must be :

- calculation of the geodesic distance function of the mask in itself,
- calculation of the geodesic distance function of voids in the complementary set of gravel (image F),
- subtraction of these two images,

- threshold between 1 and 255 (image M), (Figure 4),
- multiplication of the image F by the image M, (Figure 5).

The histogram of the distance function gives the geodesic distance distribution. Then the same parameters as before are performed.

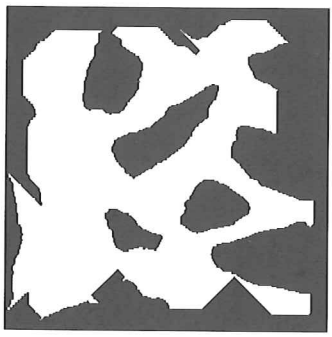

Figure 4 : Adaptative mask.

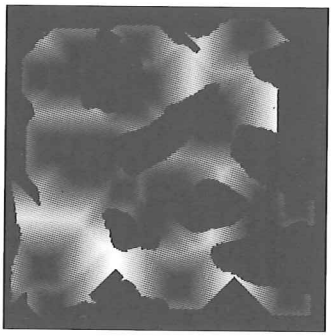

Figure 5 : Geodesic distance function in the mask.

RESULTS

For each analysis method, a graph of the distance distribution and its histogram are given. Graphs for batch A are presented in figures 6 to 9. This batch is used to compare the different methods themselves.

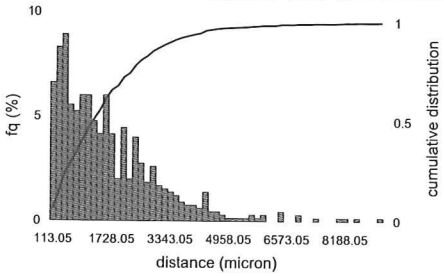

Figure 6 : Distribution of distances for the batch A with the geodesic method by individual analysis.

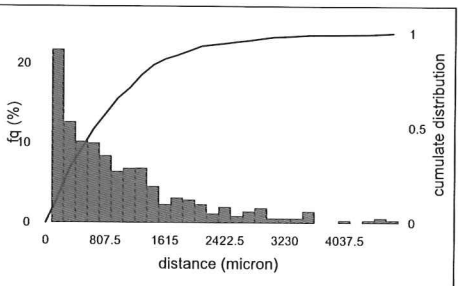

Figure 7 : Distribution of distances for the batch A with the geodesic count-dilation method.

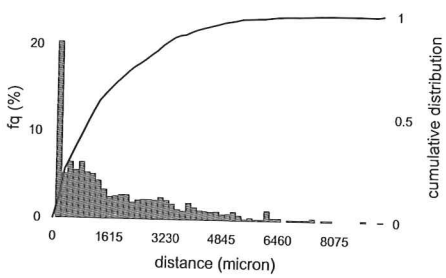

Figure 8 : Distribution of distances for the batch A by the geodesic SKIZ method.

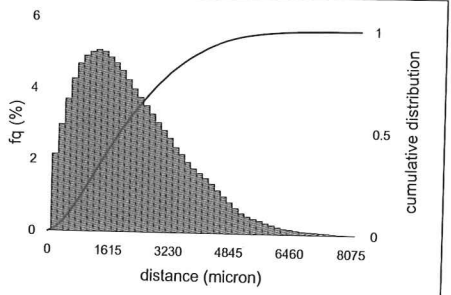

Figure 9 : Distribution of distances for the batch A by the geodesic distance function.

DISCUSSION

Comparison of the different methods

To resume the results given by the different distributions, five parameters have been chosen to compare these different methods :

- the mean distance, d_m,
- the standard deviation, σ,
- the median of the cumulative distribution, $d_{0.5}$,
- the first and third quartile, σ_1, σ_2,
- its value at 95 %, $d_{0.95}$.

These results are given in Table III.

Table III : Results of the different methods for batch A, (Δd_m = 0.03 mm).

	half-distance between nearest neighbours				half-distance between neighbours (SKIZ)		distance from a point of the matrix to a void	
	individual analysis		global analysis		eucl	geo	eucl	geo
	eucl	geo	eucl	geo				
$d_{m\ mm}$	0.79	0.89	0.81	0.92	1.63	1.71	3.43	2.13
$d_{0.5}/d_m$	0.80	0.83	0.76	0.63	0.86	0.58	0.85	0.86
σ/d_m	0.85	0.87	0.84	0.96	0.69	0.99	0.66	0.65
σ_1/σ_2	0.71	0.71	0.78	0.68	0.93	0.52	0.79	0.75
$d_{0.95}/d_m$	2.4	2.9	2.2	2.5	2.1	2.7	2.2	2.1
	method 1		method 2		method 3		method 4	

For geodesic or euclidean analysis, mean values are not comparable as they depend on the methods, because the nature of distances are very different. The two first methods give the lower values : only the half-distance between the nearest neighbour is considered. The third method gives an intermediate value : the result corresponds to the mean distance between all the neighbours from one void. Finally, the distance function considers all point

of the matrix including the distances of the farest points. So its mean value is greater than the others.

The individual analysis and the count-dilation method must give comparable results. We see that they are really similar (Table III).

Now we can compare the two types of analysis for a same method : the euclidean and the geodesic way. For the distance between nearest neighbours and all neighbours, the geodesic mean values are higher than that obtained by the euclidean process. That corresponds, in fact, to the right way of the definition of the geodesic distance. However, the difference between these two values (euclidean and geodesic) is small (2 to 4 pixels; 1 pixel ≡ 31.75 μm). This small difference can be explained from three arguments. The gravel delimits some range in the image where the air-voids are grouped together. So, even in an euclidean way, the neighbour of a void is in its range; and generally, it is the same than in a geodesic way. Although, the sand may increase the difference between euclidean and geodesic distance, because it represents a large surface of the image and it really separates each void. Moreover, this is not always the same distance that is measured. Indeed, in the case where there is gravel between two nearest neighbour voids for the euclidean method, the nearest neighbour for the geodesic method will not be the same void (figure 10). Finally, with a square grid, the difference between euclidean and geodesic distances is very small : for this example the difference is only 5 pixels (figure 11).

For the distance function, the fact that the gravel is not taken into consideration for the euclidean results, leads to an opposite result. The gravel presents a great surface area, so, in the euclidean function, all these points are considered like matrix points, but they are not represented in the geodesic way. In consequence the euclidean mean value is higher than that given by the geodesic method. If we consider that in concrete water cannot move inside gravel, this euclidean method must be excluded.

The second parameter in Table III is the median distance/mean distance ratio ($d_{0.5}/d_m$). The mean distance is always higher than the median distance ($d_{0.5}/d_m<1$), so all distance distributions are asymmetric : although the great distances correspond to a small percentage, they have a great influence on the mean distance. This asymmetry is confirmed by the parameter σ_1/σ_2. For a same method, except for the euclidean distance function, this asymmetry is more important for the geodesic method, particularly for the third one (the SKIZ method), (Figure 8) : this method searches neighbours more distant than those given by the first and second ones.

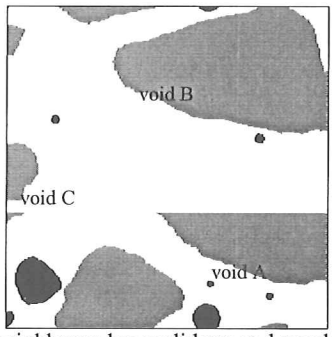

Figure 10 : Notion of neighbours by euclidean and geodesic methods : the void B is the nearest neighbour of the void A by euclidean method, but by the geodesic way it is the void C.

Finally, the values of $d_{0.95}$ are always equal to 2 to 2.9 times the mean value. The gap with the mean value is again greater for the geodesic methods, particularly for the method using the SKIZ.

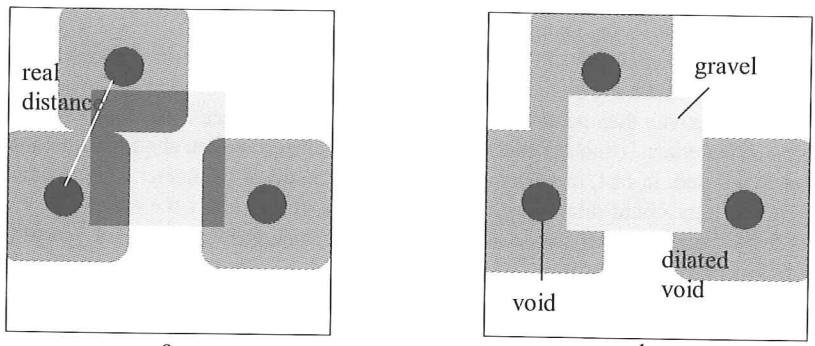

Figure 11 : Euclidean and geodesic dilation of voids in a synthetic image : the half-distance between voids by euclidean way is 36 pixels, and by the geodesic way 41 pixels.

Influence of gravel content

To estimate the influence of gravel content, we have chosen to compare the results of the different batches just for one method. Figure 12 presents the mean distance between nearest neighbours by the count-dilation method, expressed as a function of gravel content for the euclidean and the geodesic process.

We establish that this distance increases with gravel content. That appears normal because as this content increases, the air-voids number decreases (Table II). Moreover, if the evolution of the euclidean and the geodesic distance are compared, the gap between these two methods increases with gravel content. This is only due to the geodesic effect of gravel.

The evolution of the distribution of geodesic distance function with the gravel content is similar and can be explained by the same reasons. We can note however that for an algorithmic point of view, this method is the fastest used.

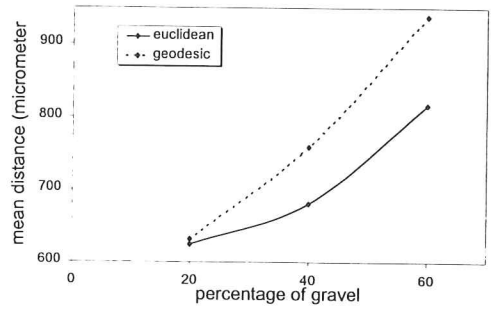

Figure 12 : Representation of the mean distance given by the count-dilation method as a function of the percentage of gravel in concrete.

CONCLUSION

The study of air-void distance distribution in concrete is important regarding the frost resistance of these material. We have then proposed four automatic methods to characterise this dispersion, using euclidean and geodesic processes.

The results show that the difference between the two types of analysis (euclidean and geodesic) is small. However, according to a physical point of view, the water cannot move through gravel, then geodesic distances appear more correct. From this work and for this type of materials, it appears that the euclidean distance function should not be the best method to be used. In fact, if we want to study the normalized parameter (the half-distance between void), the count-dilation method is preferable. But to study the way that the water has to cover from a random point of the matrix to a void, the dispersion of the geodesic distance function is preferable.

ACKNOWLEDGEMENTS

This work was performed in the frame of the "Pôle Traitement et Analyse d'Images", Pôle TAI, of Basse-Normandie, France. One of the author (ASD) is supported by the Ministère de l'Education Nationale, de la Recherche et de la Technologie.

Specimens were elaborated at ESITC, Groupe ESTP, Caen: we want to thank this establishment for its help.

REFERENCES

ATILH. Le béton exposé aux agressions hivernales. Documentation Technique n °1 janv 1989.

Coster M, Chermant JL. Précis d'analyse d'images. Paris : Les éditions du CNRS, 1985; 2nd edition. Paris : Presses du CNRS, 1989.

De Hoff RT, Rhines FN. Quantitative Microscopy. New-York : Mc Graw Hill, 1968.

Hadwiger H. Vorslesungen über Inhalt, Oberfläche und Isoperimetrie. Springer Verlag, 1957.

Kohler R. A segmentation system based on thresholding. Comput. Graphics Image Process 1981; **15** : 319-338.

Kunt M. Traitement de l'information. Vol 2 : Traitement numérique des images. Ch. 5. Presses Polytechniques et Universitaires Romanes, 1991: 142-163.

Lantuejoul C, Beucher S. On the use of geodesic metric in image analysis. J Microscopy 1981; **121** : 33-49.

Mielenz RC, Wolkodoff VE, Backstrom JE, Flack HL. Origin, evolution, and effect of air void system in concrete. Part 1-Entrained air in unhardened concrete. Proceedings, American Concrete Institute 1958; **55** : 95-121.

Pigeon M, Lachance M. Critical air-void spacing factors for concretes submitted to slow freeze-thaw cycles. Amer Concr Inst J 1981; **78**, n° 4 : 282-291.

Powers TC. The air requirement of frost resistant concrete. Proceedings of the Highway Research Board 1949; **29** : 184-211.

Powers TC, Helmuth RA. Theory of volume changes in hardened cement paste during freezing. Proceedings of the Highway Research Board 1953; **32** : 285-297.

Powers TC. Void spacing as a basis for producing air-entrained concrete. J Amer Concr Inst 1954; **50** : 741-760.

Rosenfeld A, Pfaltz JL. Distance functions on digital pictures. Pattern Recognition 1968; **1** : 33-61.

Serra J. Image Analysis and Mathematical Morphology. New-York : Academic Press, 1982.

Shehata MT. Application of image analysis in characterising dispersion of particles. In : Petrucks W, ed. Ottawa, Canada. Mineralogical Association of Canada, 1989; **16**, Ch 14 : 119-132.

Whiting D, Stark D. Control of air content in concrete. National Cooperative Highway Research Program Report N° 258. Transportation Research Board, Washington, DC, 1983.

Presented at the 7th European Congress for Stereology, Amsterdam, April 20th to 23rd, 1998.